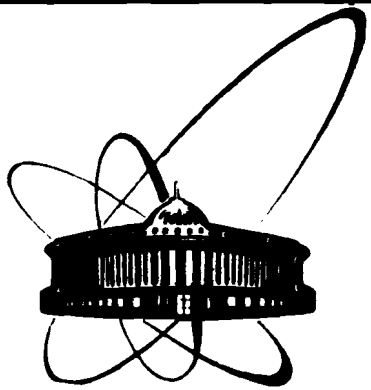

объединенный
институт
ядерных
исследований
дубна

E2-89-829

Yu.P.Ivanov, A.A.Osipov, M.K.Volkov

THE DECAY $\tau \to 3\pi\nu_\tau$ AND CHARACTERISTICS OF a_1 MESON

Submitted to "Zeitschrift für Physik C -
- Particles and Fields"

1989

1. Introduction

During the last decade different collaborations [1-6] have carried out programmes aimed at measuring the parameters of the axial-vector a_1 meson ($I^G J^{PC} = 1^- 1^{++}$). Two groups of processes essentially differing in their physical nature were studied. These are the hadronic reactions $\pi^- N \to 3\pi N$ [1,2] and the semileptonic decays $\tau \to 3\pi \nu_\tau$ [3-6]. Despite the good statistics, the data on the mass and width of the a_1 meson obtained from these processes greatly differ (see table 1). Possible reasons for this discrepancy are discussed in the literature [7-10].

The reaction $\tau \to 3\pi \nu_\tau$ is more preferable from the point of view of the extraction of the a_1 meson parameters. In this case there is no kinematic coherent background, and the transition caused by the weak axial-vector hadronic current can be described by a resonant formula of the Breit-Wigner type. It contains all information on the interaction of decay products and has a pole corresponding to the a_1 meson contribution.

It is clear that the extracted characteristics of this wide resonance depend on the analytic form of the function used in the analysis of the experimental data. Now the modifications of the Breit-Wigner formula, which are reduced to natural attempts to take into account the dependence of the a_1 resonance width on the effective mass of the three-pion system, are discussed [7-9]. They allow the agreement of a_1 meson mass values obtained from hadron and lepton processes. Yet, the a_1 meson width extracted from lepton processes is much larger.

In this situation we believe it to be important to use modern theoretical models for construction of functions of the Breit-Wigner type. Unlike earlier approaches [11,12], they allow more profound information on the structure of meson vertices and on interaction of the decay products. An attempt of this kind are papers [9,13-15].

To perform the necessary calculatios in this paper, we use the quark model of superconductivity type (QMST) [16]. The Lagrangian of the model is a generalisation of the well-known Lagrangian proposed by Nambu and Jona-Lasinio [17]. Recently, many papers have appeared, where its relation with QCD is discussed [18] and possible models of low energy meson physics based on it are considered [16,19,20]. The QMST is one of them.

Unlike the earlier approaches, ours are concentrated on the study of the $a_1 \to \pi\rho$ meson vertex structure based on its connection with a number of related processes, e.g. the radiative decays $a_1 \to \pi\gamma$ and $\pi \to e\nu\gamma$. This universal approach allows more profound information on the structure of this vertex. So we follow the principle of the minimal changes in the standard formulae used for the analysis of the experimental data in [3-6].

2. Axial-vector current $J^\mu(a_1 \to 3\pi)$ in QMST

The matrix element of the $\tau^- \to 3\pi\nu_\tau$ decay is of the form

$$T_{\tau\to 3\pi\nu_\tau} = i g_\rho^2 F_\pi G_F \cos\theta \; [\bar{\nu}_\tau(p')\gamma_\mu(1-\gamma_5)\tau(p)] f^\mu(q_1,q_2|q_3). \qquad (1)$$

The constant g_ρ describes the $\rho \to \pi\pi$ decay and is equal to $g_\rho^2/4\pi = \alpha_\rho \cong 3$, G_F is the Fermi constant, θ is the Cabibbo angle, $F_\pi = 93$ MeV, q_1, q_2 are the momenta of the π mesons carrying the same charge, q_3 is the momentum of the third pion.

The weak hadronic current $f^\mu(q_1,q_2|q_3)$ is simply related to the $a_1 \to \pi\pi\pi$ current $J^\mu(q_1,q_2|q_3)$ as

$$f^\mu(q_1,q_2|q_3) = \frac{m_{a_1}^2 g^{\mu\nu} - Q^\mu Q^\nu}{m_{a_1}^2 - Q^2} J^\mu(q_1,q_2|q_3). \qquad (2)$$

The decay width is calculated by the formula [21]

$$d\Gamma = \frac{(G_F \cos\theta)^2}{16\pi m_\tau^3} (m_\tau^2 - s)^2 \left[(m_\tau^2 + 2s)\rho_t(s) + m_\tau^2 \rho_l(s)\right] ds, \qquad (3)$$

where $s = Q^2$ takes the values in interval $0 \le s \le m_\tau^2$. The transverse $\rho_t(s)$ and longitudinal $\rho_l(s)$ spectral densities are determined from the formulae

$$\rho_l(s) = 8\pi(\alpha_\rho F_\pi)^2 (2\pi)^4 \delta^4\Big(Q - \sum_{i=1}^{3} q_i\Big) \frac{(Qf)(Qf)^+}{Q^4} \prod_{i=1}^{3} \left[\frac{d^3\vec{q}_i}{(2\pi)^3 2E_i}\right], \qquad (4)$$

$$\rho_t(s) = 8\pi(\alpha_\rho F_\pi)^2 (2\pi)^4 \delta^4\Big(Q - \sum_{i=1}^{3} q_i\Big) \frac{1}{3Q^2}\left[\frac{(Qf)(Qf)^+}{Q^2} - ff^+\right] \prod_{i=1}^{3} \left[\frac{d^3\vec{q}_i}{(2\pi)^3 2E_i}\right].$$

When determining the spectral density function, we shall use the hadronic current J^μ which, according to (2), allows calculation of the scalar products

$(Qf) = (QJ)$,

$$\left[\frac{(fQ)(fQ)^+}{Q^2} - ff^+\right] = \frac{m_{a_1}^2 (m_{a_1}^2 + \Gamma_{a_1}^2)}{(m_{a_1}^2 - Q^2)^2 + m_{a_1}^2 \Gamma_{a_1}^2} \left[\frac{(JQ)(JQ)^+}{Q^2} - JJ^+\right]. \qquad (5)$$

It is seen that the spectral density $\rho_t(s)$ has a typical Breit-Wigner form

$$\rho_t(s) = \frac{2}{\pi(g_\rho Z)^2 \sqrt{s}} \left[\frac{m_{a_1}^2 (m_{a_1}^2 + \Gamma_{a_1}^2)}{(m_{a_1}^2 - s)^2 + m_{a_1}^2 \Gamma_{a_1}^2}\right] \Gamma_{a_1\to 3\pi}(s), \qquad (6)$$

where

$$\Gamma_{a_1\to 3\pi}(s) = (2\pi)^4 \left[\delta^4\Big(Q - \sum_{i=1}^{3} q_i\Big) \frac{(g_\rho^3 F_\pi Z)^2}{12\sqrt{s}} \left[\frac{(JQ)(JQ)^+}{Q^2} - JJ^+\right] \prod_{i=1}^{3} \left[\frac{d^3\vec{q}_i}{(2\pi)^3 2E_i}\right]\right.$$

is the decay width of the resonant a_1 state for the case when the axial meson is off the mass shell ($s=Q^2$).

The main contribution to the hadronic current J^μ will come from the decay channel $a_1 \to \pi\rho \to 3\pi$. In this aproximation we have

$$J'^{\mu}(q_1,q_2|q_3) = \left\{ g^{\mu\nu} - \frac{2Q^\mu Q^\nu}{Q^2} + \frac{1}{m^2_{a_1}}\left[(q^2_{13}-Q^2)g^{\mu\nu}+Q^\mu Q^\nu\right] + \right.$$

$$\left. + \frac{1}{8\pi^2 F_\pi^2 Z}\left[(q^2_{13}-q_{13}q_2)g^{\mu\nu}+q_2^\nu q^\mu_{13}\right]\right\} \frac{(q_1-q_3)^\nu}{m^2_\rho - q^2_{13} - i m_\rho \Gamma_\rho} + (1\leftrightarrow 2), \qquad (7)$$

Here $Q=q_1+q_2+q_3$, $q_{13}=q_1+q_3$, $q_{23}=q_2+q_3$, $\Gamma_\rho=153$ MeV is the ρ meson width. The constant Z results from taking into account the $\vec{a}_1 \to \partial\vec{\pi}$ transitions and is equal to $Z=(1-6m^2/m^2_{a_1})^{-1}$ [22], where m is the mass of the constituent u quark. We shall use another expression for it as well. It can be obtained from the previous formula if one uses the relations $Z^{1/2} g_\rho = \sqrt{6} g$ and $g=m/F_\pi$ [23].

$$Z^{-1} = \frac{1}{2}\left[\, 1+\sqrt{1-(2g_\rho F_\pi / m_{a_1})^2}\,\right]. \qquad (8)$$

In formula (7) the expression in braces corresponds to the $a_1\pi\rho$ vertex. Let us consider it more thoroughly. There are three diagrams which contribute to the amplitude of this process (see fig 1). They lead to the following expression

$$T_{a_1^-\to\pi^-\rho^0} = -ig_\rho^2 F_\pi Z\, \varepsilon_\mu(Q)\varepsilon_\nu(q)\left\{ g^{\mu\nu} - \frac{2Q^\mu Q^\nu}{Q^2} + \frac{1}{m^2_{a_1}}\left[(q^2-Q^2)g^{\mu\nu}+Q^\mu Q^\nu\right] + \right.$$

$$\left. + \frac{1}{8\pi^2 F_\pi^2 Z}\left[(q^2-qk)g^{\mu\nu}+k^\nu q^\mu\right]\right\}. \qquad (9)$$

Here k,q are the momenta of the pion and the ρ meson, $Q=k+q$, $\varepsilon_\mu(Q)$ and $\varepsilon_\nu(q)$ are the polarisation vectors of the a_1 and ρ mesons. Since $m_\pi^2 \ll m_\rho^2, m^2_{a_1}$, we consider that $k^2=m_\pi^2=0$. We keep the terms

proportional to Q^μ, which are necessary for consideration of the processes with the virtual a_1 meson, though in this case their contribution is equal to zero.

The first amplitude terms in formula (9) correspond to the vertices of phenomenological chiral Lagrangian [24] and are obtained from diagrams 1a, 1c and 1b respectively. The last term (in the second pair of brackets) appears as a result of the q^2 expansion of the triangle quark diagram in fig 1a (where we confine ourselves to the terms to powers below two in particle momenta). This term is not the direct consequence of the use of the standard phenomenological chiral Lagrangian. Yet, it plays an important role in description of many physical processes and leads to reasonable numerical estimations, which indirectly confirms the correctness of the form obtained for it. Let us indicate some of these results.

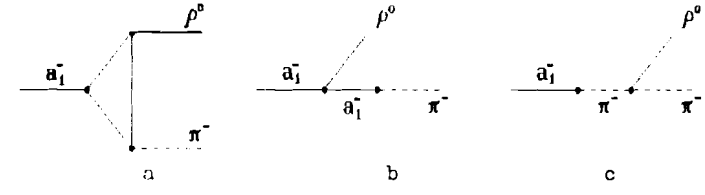

Fig 1. Diagrams, describing the $a_1\to\pi\rho$ vertex. The $a_1\to\partial\pi$ transitions are taken into account.

Using the Lagrangian

$$L_{em} = \frac{e}{g_\rho} A^\mu \cdot [m^2_\rho \rho_\mu + \frac{1}{3} m^2_\omega \omega_\mu - \frac{\sqrt{2}}{3} m^2_\varphi \varphi_\mu], \qquad (10)$$

one can easily obtain the radiative $a_1\to\pi\gamma$ decay amplitude from the $a_1\to\pi\rho^0$ amplitude; it must meet the requirement of the gradient invariance. The mechanism that ensures the fulfilment of this

requirement consists in compensation for the thus undesired first term of formula (9) by the corresponding term resulted from the diagram of fig 1b (the third term of formula (9), where $Q^2=m^2_{a_1}$). The remaining quantity is proportional to $q^2/m^2_{a_1}$ and disappears on the photon mass shell $q^2=0$. Thus, if we want amplitude (9) to lead to description of the radiative decay of a_1 as well, we must take into account the final terms of the diagrams considered. In this case the decay width $\Gamma_{a_1\to\pi\gamma}$=410 KeV (m_{a_1}=1260 MeV), which agrees with the experimental data $\Gamma^{exp}_{a_1\to\pi\gamma}$=640±246 KeV [25]. It is completely determined by the factor at the last term in (9).

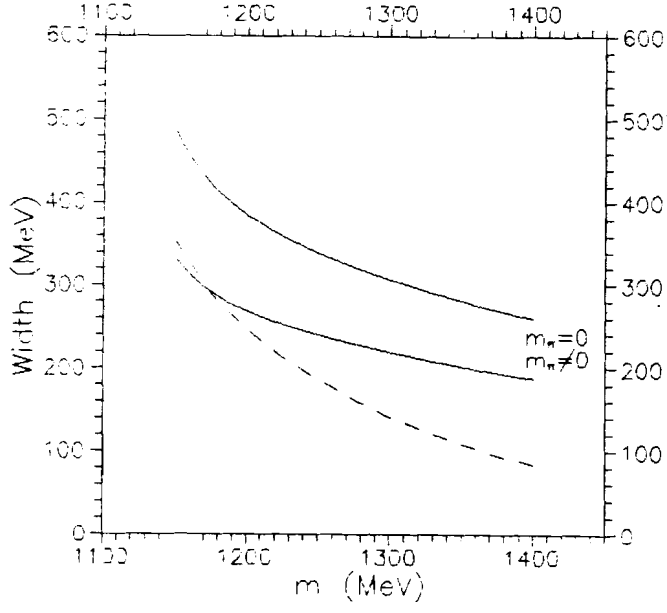

Fig 2. The widths of the $a_1\to\pi\rho$ (dotted line) and $a_1\to\pi\pi\pi$ (solid line) decays as the function of a_1 meson mass. $\Gamma(a_1\to\pi\pi\pi)$ is calculated for the two cases: $m_\pi=0$ and $m_\pi\neq0$.

Noteworthy is that the term considered is necessary in the self-consistent phenomenological description of the processes $a_1\to\pi\gamma$, $a_1\to\pi\rho$, $\pi\to e\bar{\nu}\gamma$ and in this sense it is independent of any model approach resulting only from the general considerations of gradient invariance [26].

At last, in the description of the $\pi\to e\bar{\nu}\gamma$ decay [27] by means of the last term of amplitude (9) one can obtain the axial form factor value satisfying both the experimental data and the results of other theoretical models (e.g. algebra of currents).

The hadronic current (7) allows one to calculate the width of the a_1 meson decay $\Gamma(a_1\to3\pi)$ as a function of its mass. The curve of this function is shown in fig 2. It qualitatively differs from the known result of ref [15] where $\Gamma(a_1\to3\pi)$ increases with m_{a_1} *). The discrepancy is due to the fact that in this case the curve shape is greatly affected by the final terms of the quark triangle diagram corresponding to the $a_1\pi\rho$ vertex. Note that the similar dependence was also obtained by the authors of ref [9] who took into account the form factors of meson vertices.

Axial-vector current (7) in the low-energy limit, i.e. in the approximation limited to the first terms of the expansion in particle momenta (the soft pion case), has the form

$$J'^{\mu}_{chir}(q_1,q_2|q_3) = \frac{1}{m_\rho^2}\left[g^{\mu\nu}-2\frac{Q^\mu Q^\nu}{Q^2}\right](Q-3q_3)_\nu \ . \qquad (11)$$

*) In our case it reaches its maximum at point $m_{a_1}=2g_\rho F_\pi$=1140 MeV where, as shown in [23], the low-energy Weinberg ($m^2_{a_1}=2m^2_\rho$) and KSFR relations ($m^2_\rho=2g^2_\rho F^2_\pi$) are valid.

Obviously, it is not conserved. The result agreeing with the requirements of low-energy theorems will be obtained if we consider the contributions of all the diagrams in fig 3 taken together. This problem was thoroughly studied in our separate paper [23]. For instance, it was shown there that in the low-energy limit the full hadronic current agrees with the one obtained in [13]. It is significant that this directly results from inclusion of $\vec{a}_1 \to \partial\vec{\pi}$ transition effects. Below, to avoid complications, we shall not take into account either the diagram with the ε meson or the vertices corresponding to the four-pion diagrams. The estimations show that in this case the total error will be of the order of 10% of the main contribution.

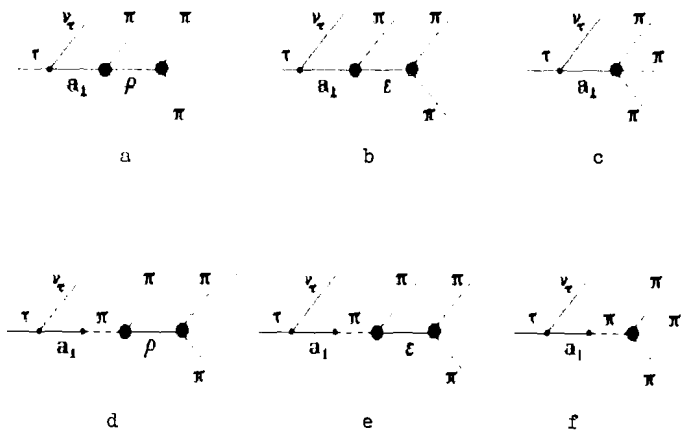

Fig 3. Feynman diagrams for the decay $\tau \to 3\pi\nu_\tau$. The bold-faced point indicates that the $a_1 \to \partial\pi$ transitions are taken into account in the corresponding vertices.

3. Results of fits to experiment

Now let us determine the mass and width of the a_1 meson. We shall use the DELCO [3], MARK II [4] and ARGUS [5] data. The basic formulae are given in (3)-(6). It should be mentioned that we ignored the pion mass, when obtaining J_μ in (7). Yet, calculating the phase volume, one must take into account the pion mass. It can be seen, for example, from fig 2. To better understand how non-locality of the $a_1\pi\rho$ meson vertex affects the final result, we shall make two preliminary estimations. First, we fit the data [3-5] using the current from (7) in the low-energy limit, i.e. when the $a_1\pi\rho$ vertex has the simplest local structure:

$$J'^{\mu}_{\lim}(q_1,q_2|q_3) = \left\{g^{\mu\nu} - \frac{2Q^\mu Q^\nu}{Q^2}\right\} \frac{(q_1-q_3)^\nu}{m_\rho^2 - q_{13}^2 - i m_\rho \Gamma_\rho} + (1\leftrightarrow 2). \qquad (12)$$

As was to be expected, the result looks like the one obtained in [3-5] (see tables 1 and 2).

If the internal structure of the main meson vertex $a_1\pi\rho$ is taken into account, i.e. formula (7) is used for fitting the data, we shall get the a_1 meson mass value that agrees with the data of the hadronic experiments. But its width turns out to be large enough and lies in the interval 400-550 MeV (see the second lines of table 2).

To compare our results with the experimental data, one must convolute the theoretical formulae with the detector resolution function [9].

$$d\Gamma^{obs}_{\tau\to\nu_\tau 3\pi}/ds = \frac{1}{m}\int_{-\infty}^{+\infty} dm' \frac{m'}{\sqrt{2\pi}\,\sigma(m')} \exp\left\{-\frac{1}{2}\left[\frac{m-m'}{\sigma(m')}\right]^2\right\} \frac{d\Gamma^{theor}_{\tau\to\nu 3\pi}}{ds'}, \qquad (13)$$

where $m = \sqrt{s}$, $m' = \sqrt{s'}$, $\sigma(m') = A + Bm'$ and A, B are the constants. At this stage the extracted value of the a_1 meson width decreases.

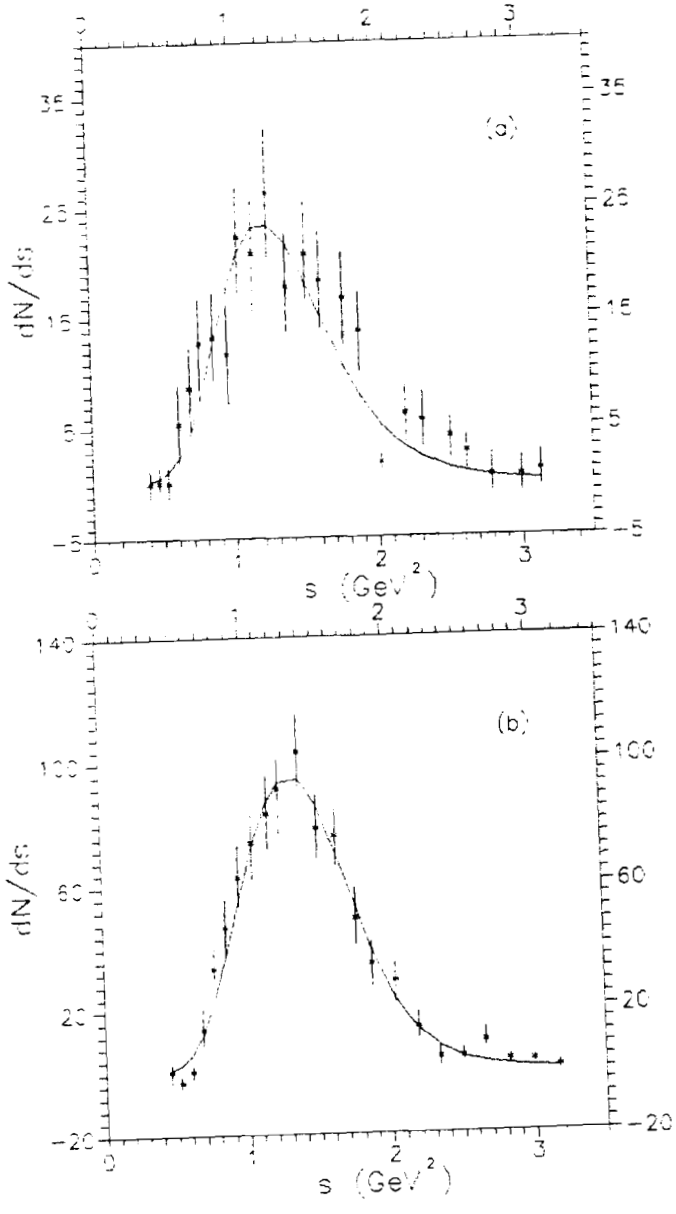

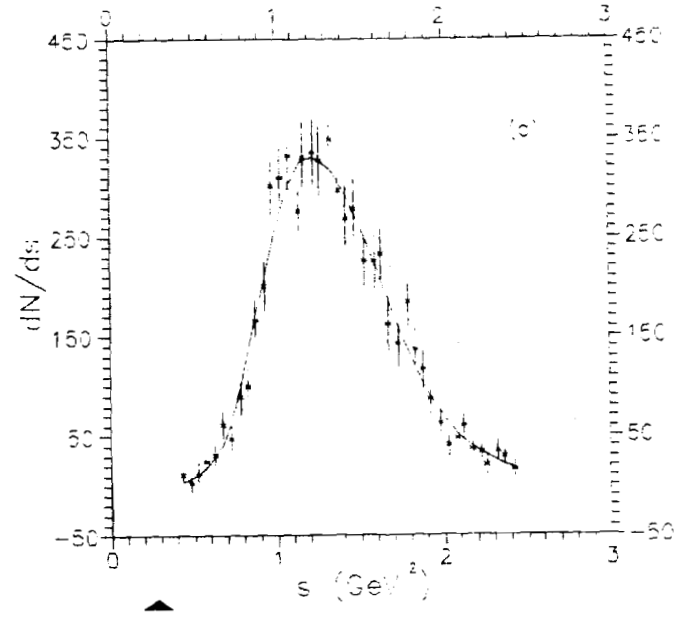

Fig 4. Fits to experimental three-pion mass spectra from $\tau \to \nu_\tau \pi^- \pi^- \pi^+$. The theoretical curves have been convoluted with a detector resolution function via eq.(13). The values of A and B are taken from Ref.[9] and equal to: (a) DELCO [3]; A=0.0 GeV, B=0.065; (b) MARK II [4]; A=0.0 GeV, B=0.065; (c) ARGUS [5]; A=0.0 GeV, B=0.030.

The situation is summed up in table 2 and fig 4, where we show the results and qualities of various fits. Note that the contribution of the longitudinal component is small and equals ~6% according to our estimations.

When speaking about the experimental data of the three collaborations in question, one should stress that they precisely fix the a_1 resonanse mass m_{a_1} = 1240-1260 MeV. Yet, the final

Table 1. The a_1 parameters, obtained by different collaborations

Source	Mass (MeV)	Width (MeV)
$\pi^- p \to p\pi^+\pi^-\pi^-$ [1]	1280±30	300±50
$\pi^- p \to n\pi^+\pi^-\pi^0$ [2]	1240±80	380±100
DELCO [3]	1056±20±15	476^{+132}_{-120}±54
MARK II [4]	1194±14±10	462±56±30
ARGUS [5]	1046±11	521±27
MAC [6]	1166±18±11	405±75±25

Table 2. The a_1 meson parameters and the χ^2/N (N-number of points) values, obtained as a result of the experimental data fit with axial-vector current (12) (the first line); with axial-vector current (7) (the second line); with axial-vector current (7) and formula (13) (the third line).

Data	Mass (MeV)	Width (MeV)	χ^2/N	$Br(\tau \to \nu_\tau \pi^-\pi^-\pi^+)$
DELCO [3]	1092±70	656±193	28/24	2.4±1.0 %
	1261^{+46}_{-28}	537^{+207}_{-131}	28/24	2.6±0.8 %
	1242±37	465^{+228}_{-143}	27/24	3.0±1.2 %
MARK II [4]	1175±15	459^{+64}_{-51}	36/23	4.3±0.8 %
	1285^{+21}_{-18}	426±56	32/23	3.6±0.6 %
	1260±14	298^{+40}_{-34}	32/23	5.3±0.8 %
ARGUS [5]	1115±10	524^{+41}_{-37}	38/41	3.3±0.3 %
	1255^{+9}_{-10}	525^{+40}_{-36}	37/41	2.7±0.2 %
	1250±9	488±32	39/41	2.9±0.3 %

conclusion on the a_1 meson width requires more investigations. The points obtained by ARGUS yield Γ_{a_1}=488±32 MeV, while the DELCO data ($\Gamma_{a_1}=465^{+228}_{-143}$ MeV) do not exclude the value Γ_{a_1}=316±45 MeV, mentioned earlier by the Particle Data Group. The MARK II data ($\Gamma_{a_1}=298^{+40}_{-34}$ MeV) are in complete agreement with the results of hadronic experiments. From the point of view of the QMST the lower values of the a_1 width are preferred (see fig 2). In this sense the fits of the MARK II data match the model best.

In our analysis we have made the least possible changes in the standard formulae used in [3-6]. These changes were connected with the $a_1\pi\rho$ vertex. At present a number of other effects that can affect the value of the a_1 resonance parameters are discussed in publications. Among them there are

a) New vertices like those shown in figs 3b,c,e,f.

b) s-dependence of a_1 meson mass in the propagator.

c) $K^*\bar{K} + \bar{K}^*K$ thresholds.

d) Contribution from the radially excited state (a_1') of the a_1 meson.

We believe that all these questions can be a topic of further investigations of the a_1 meson within the framework of the QMST.

Acknowledgements

We wish to thank B.Z.Kopeliovich and A.Pich for discussions.

References

1. C.Daum et al.: Nucl.Phys. B182 (1981) 269
2. J.Dankowych et al.: Phys.Rev.Lett.46 (1981) 580

3. W.B.Rückstuhl et al.(DELCO): Phys.Rev.Lett.56 (1986) 2132
4. W.B.Schmidke et al.(Mark II): Phys.Rev.Lett.57 (1986) 527
5. H.Albrecht et al.(ARGUS): Z.Phys.C - Particles and Fields 33 (1986) 7
6. H.R.Band et al.(MAC): Phys.Lett. 198B (1987) 297
7. M.G.Bowler: Phys.Lett. 182B (1986) 400
8. N.A.Törnqvist: Z.Phys.C - Particles and Fields 36 (1987) 695
9. N.Isgur, C.Morningstar, C.Reader: Phys.Rev. D39 (1989) 1357
10. J.Iizuka, H.Koibuchi, F.Masuda: Phys.Rev. D39 (1989) 3357
11. Y.S.Tsai: Phys.Rev. D4 (1971) 2821
12. W.R.Frazer, J.R.Fulco, F.R.Halpern: Phys.Rev. B136 (1964) 1207
13. R.Fischer, J.Wess, F.Wagner: Z.Phys.C - Particles and Fields 3 (1980) 313
14. H.Kuhn, F.Wagner: Nucl.Phys. B236 (1984) 16
15. T.Berger: Z.Phys.C - Particles and Fields 37 (1987) 95
16. M.K.Volkov: a) Ann.Phys. 157 (1984) 282;
b) Sov.J.Part.Nucl. 17 (1986) 433
17. Y.Nambu, G.Jona-Lasinio: Phys.Rev. 122 (1961) 345
18. A.Dhar, S.R.Wadia: Phys.Rev.Lett. 52 (1984) 959;
A.Dhar, R.Shankar, S.R.Wadia: Phys.Rev. D31 (1985) 3256;
R.D.Ball: Proceedings of the Workshop on "Skyrmions and Anomalies" eds. M.Jezabek and M.Praszalowicz, World Scientific, Singapore (1987);
N.I.Karchev, A.A.Slavnov: Teor.Mat.Fiz. 65 (1985) 192;
A.Andrianov et al.: Phys.Lett. 157B (1985) 425; Yad.Fiz. 43 (1986) 983, Teor.Mat.Fiz 70 (1987) 1;
Ulf-G.Meissner: Phys.Reports 161 (1988) 213

19. T.Eguchi: Phys.Rev. D14 (1976) 2755;
T.Kugo: Progr.Theor.Phys. 55 (1976) 2032;
K.Kikkawa: Progr.Theor.Phys. 56 (1976) 947;
H.Kleinert: Fortschr.der Phys. 26 (1978) 565
20. D.Ebert, M.K.Volkov: Yad.Fiz. 36 (1982) 1265;
Z.Phys.C - Particles and Fields 16 (1983) 205
21. L.B.Okun: Leptons and Quarks (North-Holland, Amsterdam, 1982)
22. M.K.Volkov, A.A.Osipov: JINR Communication P2-85-390 Dubna (1985).
23. A.A.Osipov, M.K.Volkov: JINR Preprint E2-89-713 Dubna (1989)
24. S.Gasiorowicz, D.A.Geffen: Rev.Mod.Phys. 41 (1969) 531
25. M.Zielinsky et al.: Phys.Rev.Lett. 52 (1984) 1195
26. M.K.Volkov: Phys.Lett. 222B (1989) 298
27. A.N.Ivanov, M.Nagy, M.K.Volkov: Phys.Lett. 200B (1988) 171

Received by Publishing Department
December 14, 1989.